1.00

Imaging-Based 3D Reconstruction of Sample Mass Lost from the OSIRIS-REx Spacecraft

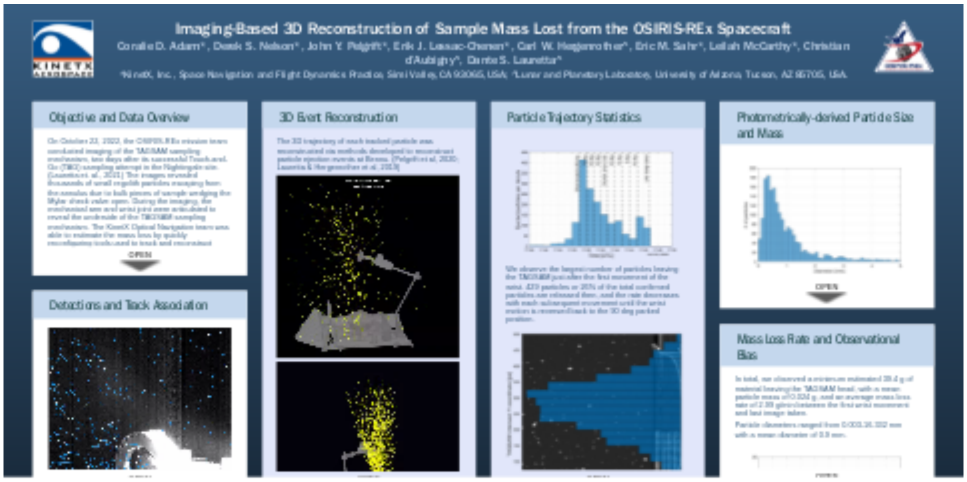

Coralie D. Adam*, Derek S. Nelson*, John Y. Pelgrift*, Erik J. Lessac-Chenen*, Carl W. Hergenrother^, Eric M. Sahr*, Leilah McCarthy*, Christian d'Aubigny^, Dante S. Lauretta^

*KinetX, Inc., Space Navigation and Flight Dynamics Practice, Simi Valley, CA 93065, USA; ^Lunar and Planetary Laboratory, University of Arizona, Tucson, AZ 85705, USA.

PRESENTED AT:

OBJECTIVE AND DATA OVERVIEW

On October 22, 2020, the OSIRIS-REx mission team conducted imaging of the TAGSAM sampling mechanism, two days after its successful Touch-and-Go (TAG) sampling attempt in the Nightingale site. (Lauretta et. al., 2021) The images revealed thousands of small regolith particles escaping from the annulus due to bulk pieces of sample wedging the Mylar check valve open. During the imaging, the mechanical arm and wrist joint were articulated to reveal the underside of the TAGSAM sampling mechanism. The KinetX Optical Navigation team was able to estimate the mass loss by quickly reconfiguring tools used to track and reconstruct Bennu's particle ejection phenomena.

[VIDEO] https://res.cloudinary.com/amuze-interactive/image/upload/f_auto,q_auto/v1639170677/agu-fm2021/62-0e-1d-4e-ea-0d-da-fb-80-b3-ef-85-fa-52-ff-9a/image/shower_head_qgn4ql.mp4

The escaping particles could be tracked across multiple images, which allowed us to detect, associate, and track particles using a combination of manual and automated techniques. The associated tracks each represent a unique particle that was further analyzed to estimate its ejection time, 3D trajectory, and velocity, as well as its photometric properties, which were used to compute its brightness, size, and mass. Compiling the aggregate photometric and physical data for all of the particles leads to an estimate of sample mass lost during the post-TAG imaging sequences, which aided in the decision to stow the sufficiently remaining sample on October 28, 2020. (Lauretta et. al., 2021) The sample will return to Earth for analysis in September 2023.

During the 10-minute post-TAG imaging activity, the wrist was articulated across 9 positions, each captured with 9 SamCam (Rizk, et al., 2018) images of varying, increasing exposure. Before the imaging began, the elbow was articulated to bring the head into the instrument field of view (FOV).

We first process the raw images to remove spurious signal from dark bias and stray light. We use a local median filter coupled with an iterative background subtraction technique (Levesque, 2008) to remove most of the remaining stray light and corresponding noise from the TAGSAM head. This results in images containing only remaining signals from the TAGSAM head, visible particles, and remaining stray light that was not subtracted during the process.

DETECTIONS AND TRACK ASSOCIATION

[VIDEO] https://res.cloudinary.com/amuze-interactive/image/upload/f_auto,q_auto/v1639179566/agu-fm2021/6a-bf-4a-a3-cb-f8-c0-c4-b8-80-72-60-fc-3c-02-cd/image/pose_1743_eric_manual_tracks_ukqilp.mp4

We build a database of detections through hybrid automated and manual techniques.

The automatic particle detection algorithm first applies a strict threshold to binarize the image and isolate particles from remaining background signal. It employs an iterative optimal clustering algorithm (Calinski, Harabasz, 1974 & Arthur, 2007) to determine the coordinates of the candidate particle detections, from which a centroid algorithm is applied to the non-binarized image. A custom GUI tool was developed to allow an analyst to manually review, add, or delete detections.

Once the detection database is populated for all images, detections are associated to one another across the image sequence using a variety of criteria. A classical multiple hypothesis tracking (MHT) algorithm (Blackman, 2004) is employed, allowing for multiple hypotheses to be stored and tested for each detection and candidate track. Exploiting the fact that most particles follow linear paths due to lack of external forces, an angle constraint is applied in the MHT.

Once all the candidate tracks are computed, additional logics are applied to reduce the dataset to only tracks that are physically possible and uniquely associated with an exclusive set of detections. We constrain the range of angular velocities to an empirically–derived threshold of 10 pixels/s, and we further constrain the range of angular accelerations to < 0.75 px/s^2 to enforce the accelerations to be approximately constant. Finally, we deconflict remaining tracks by preferring a higher coefficients of determination (R^2) from the MHT. The resulting database of tracks are used for further trajectory reconstruction and photometric analysis.

3D EVENT RECONSTRUCTION

The 3D trajectory of each tracked particle was reconstructed via methods developed to reconstruct particle ejection events at Bennu. (Pelgrift et al, 2020; Lauretta & Hergenrother et al, 2019)

[VIDEO] https://res.cloudinary.com/amuze-interactive/image/upload/f_auto,q_auto/v1639179938/agu-fm2021/6a-bf-4a-a3-cb-f8-c0-c4-b8-80-72-60-fc-3c-02-cd/image/tagsam_3d_movie_ka8dx5.mp4

[VIDEO] https://res.cloudinary.com/amuze-interactive/image/upload/f_auto,q_auto/v1639180037/agu-fm2021/6a-bf-4a-a3-cb-f8-c0-c4-b8-80-72-60-fc-3c-02-cd/image/tagsam_3d_static_zcxpmw.mp4

Assuming each track follows a linear trajectory with no external accelerations, a 3D trajectory can be determined for all tracks with 3 or more observations and a known ejection location.

The ejection location is determined by fitting a 2D line to the track in the image plane and finding the 2D intercept with an ellipse representing the TAGSAM head. The range of the TAGCAM head is well known relative to the SamCam optics for each wrist pose, based on a 3D model of the spacecraft. With the 3D ejection location determined, the 3D trajectory can be estimated based on the origin and observed angular positions. (Pelgrift et al, 2020)

In total, we tracked 1662 particles leaving the TAGSAM head. However, the nature of the FOV creates an observational bias where particles on the far side of the TAGSAM moving away from the camera persist longer in the FOV and therefore are more likely to be caught in multiple images than particles moving toward the camera.

PARTICLE TRAJECTORY STATISTICS

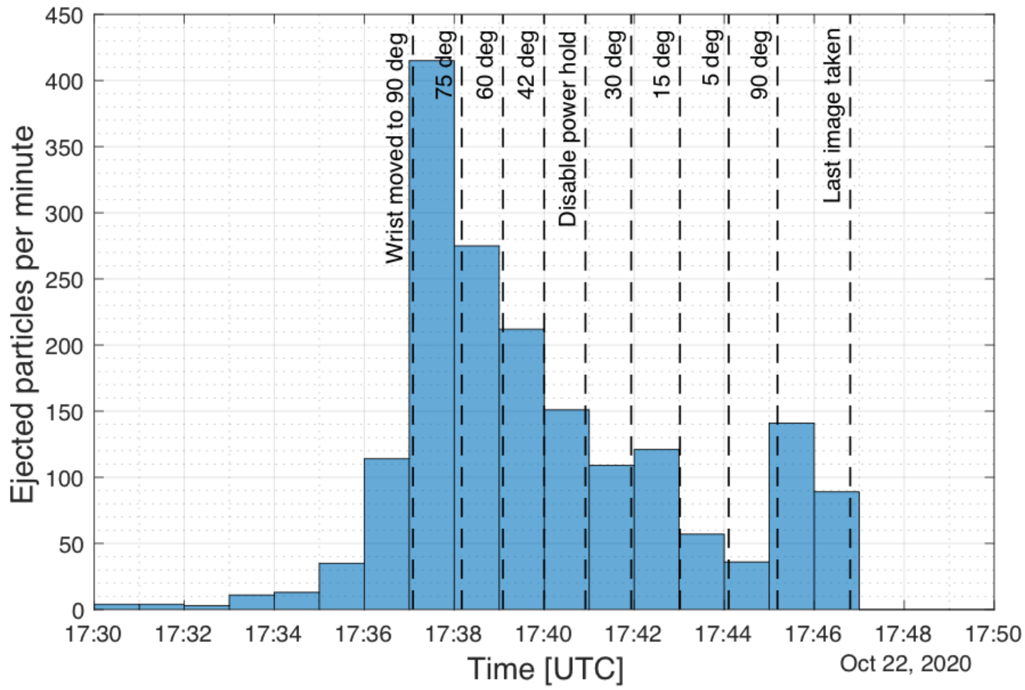

We observe the largest number of particles leaving the TAGSAM just after the first movement of the wrist. 429 particles or 26% of the total confirmed particles are released then, and the rate decreases with each subsequent movement until the wrist motion is reversed back to the 90 deg parked position.

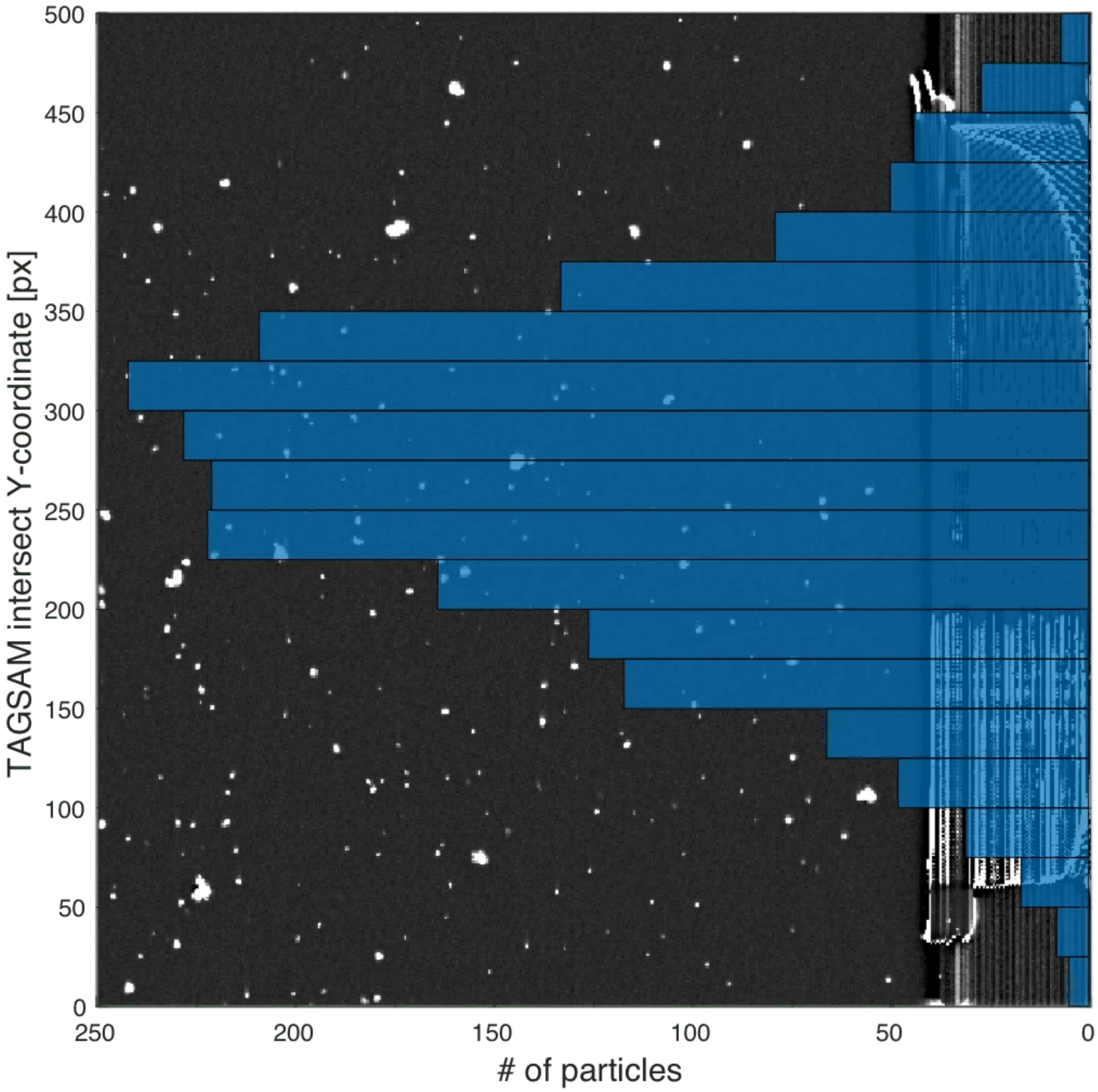

The majority of particles are released from the top half of the TAGSAM, which corresponds to the locations where the check valve appeared to be wedged open by rocks.

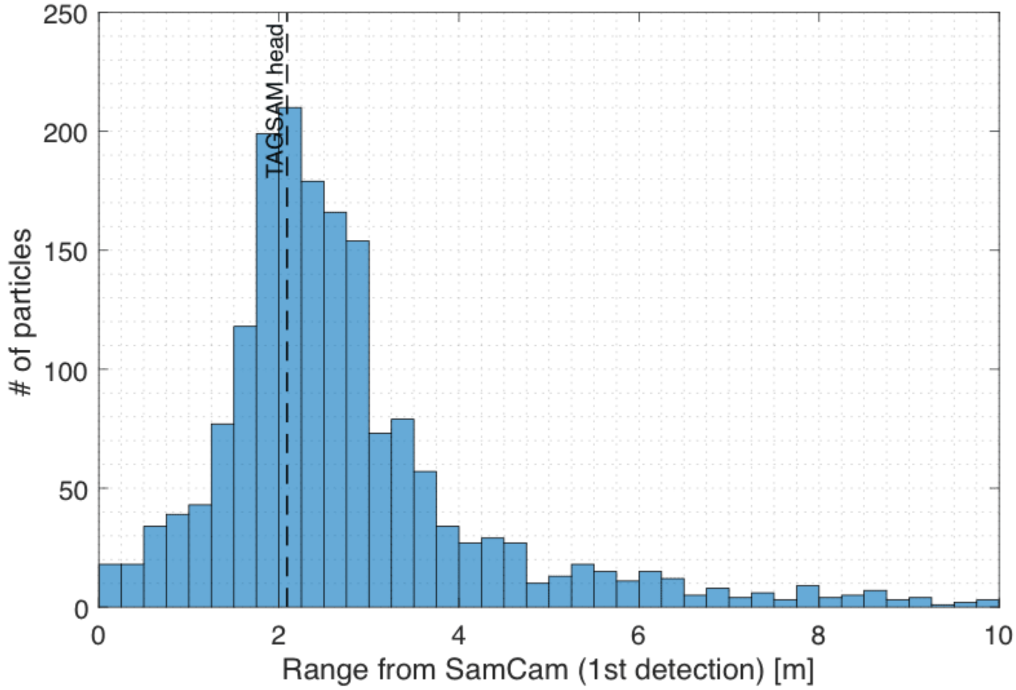

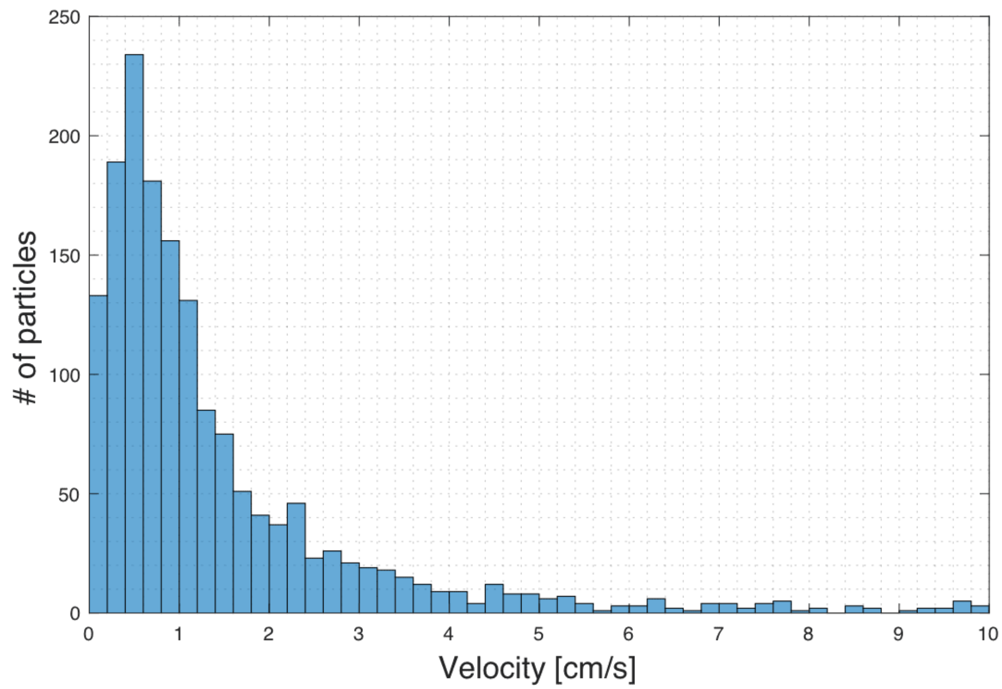

At the time of their first observation, the median estimated range from SamCam to the particles was 2.3 m. The median estimated velocity was 0.9 cm/s, and 90% of particles had velocities less than 4 cm/s

The automated detection and tracking methods are subject to some false positive detections and mis-associations of detections. Therefore, particles with an estimated velocity greater than 20 cm/s were treated as outliers and not included in the results presented here. This threshold is an order of magnitude greater than both the median particle velocity and the velocity of the TAGSAM head itself during wrist movements (roughly 0.5–1 cm/s).

PHOTOMETRICALLY-DERIVED PARTICLE SIZE AND MASS

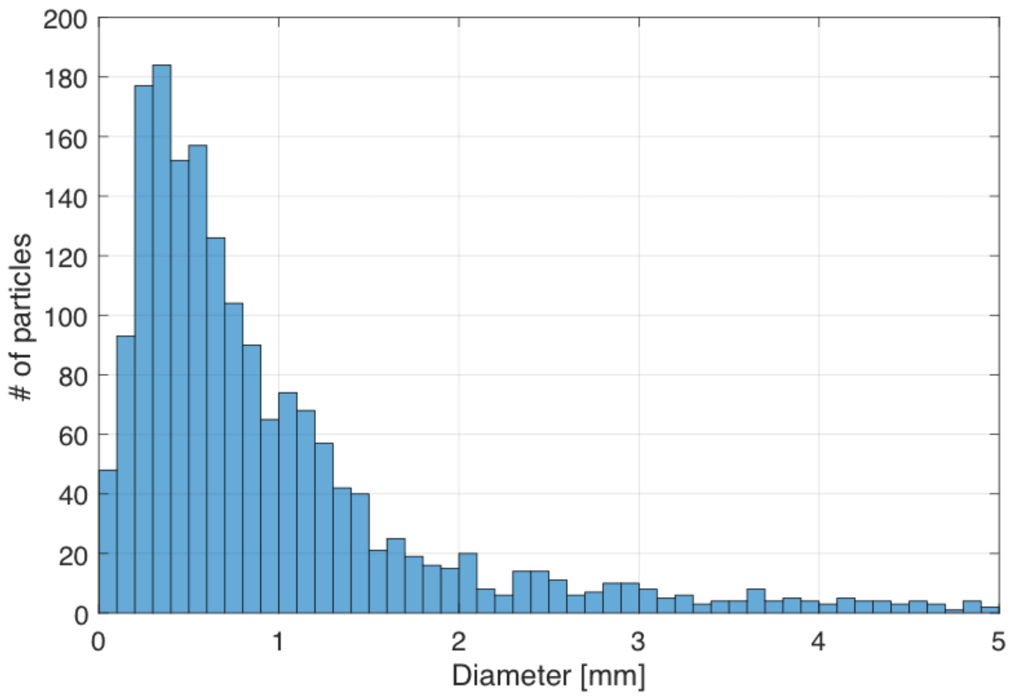

Using the 3D reconstructed trajectories to compute range and phase angle, we can photometrically estimate the size of each tracked particle.

The median particle diameter is 0.6 mm, and 95% of particles are less than 2mm.

We obtain the total signal from each tracked particle observation by integrating the fitted point spread function (PSF). This is converted to a V-band apparent magnitude by relating the apparent signal to that of a catalogued bright star in the FOV.

The absolute magnitude is computed given the estimated range and phase angle of the particle, assuming a phase coefficient of 0.013 magnitude per degree of phase angle, which was estimated by Hergenrother et al (2020) for particles ejected from the surface of Bennu.

The photometric diameter is computed from the estimated absolute magnitude by assuming the average Bennu albedo of 0.004 (DellaGiustina et al., 2019). We further assume the particles are "flake-like" ellipsoids based on the conclusions of Hergenrother et al (2020) and Chesley et al (2020) for Bennu's ejected particles, with semi-axes of $a \times a \times b$ and an axial ratio b/a = 0.27. Our reported particle diameters are based on a volume-equivalent sphere, $D = 2\sqrt{a^2 b}$. The particle masses are determined from the volumes by assuming a density of 1800 kg/m^3. (Lauretta et. al., 2021)

MASS LOSS RATE AND OBSERVATIONAL BIAS

In total, we observed a minimum estimated 39.4 g of material leaving the TAGSAM head, with a mean particle mass of 0.024 g, and an average mass loss rate of 2.99 g/min between the first wrist movement and last image taken.

Particle diameters ranged from 0.003-16.332 mm with a mean diameter of 0.9 mm.

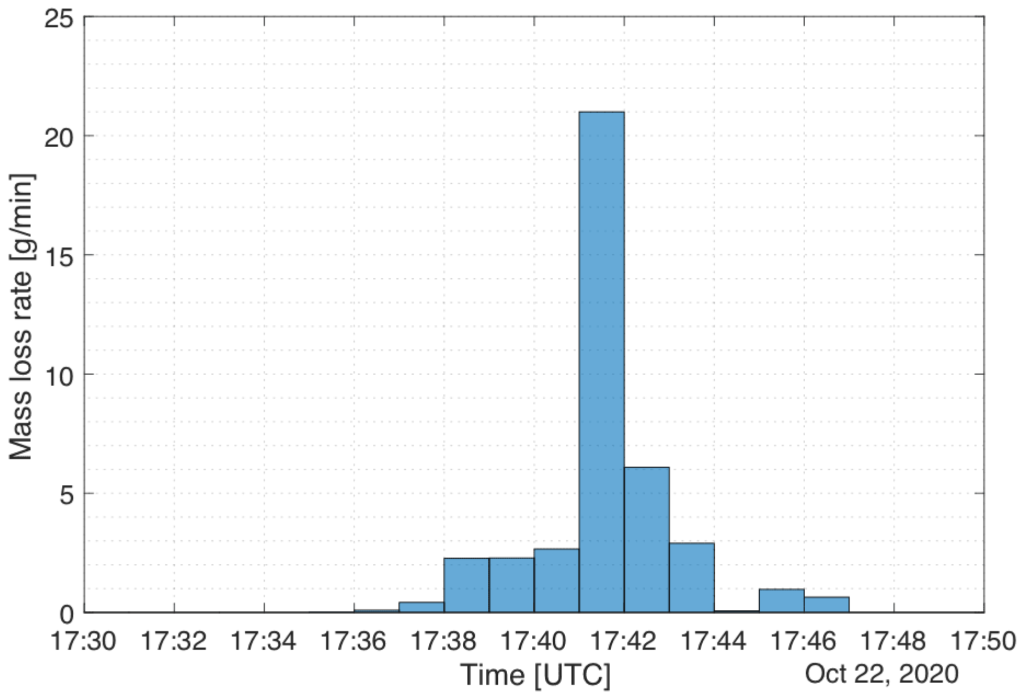

Due to the challenges of disentangling this unique data set, the particles we tracked leaving TAGSAM only represent a fraction of the particles observed in the images. Additionally, we can only compute 3D reconstructions on tracks that trace back to the TAGSAM head, which represents 39% of total tracks in the database. Thus, our results represent a lower bound of the mass loss during the post-TAG imaging activity.

ABSTRACT

On October 20, 2020, NASA's OSIRIS-REx spacecraft performed its Touch-and-Go (TAG) activity, in which it briefly contacted the surface of the asteroid Bennu and successfully collected a sample of regolith. Subsequent images of the sampling mechanism showed that thousands of small regolith particles were escaping from it, apparently in conjunction with movements of the mechanical arm and wrist joint by which the sampling mechanism is attached to the spacecraft. The escaping particles could be tracked from one image to another, and across multiple images, which allowed the OSIRIS-REx optical navigation team to detect, associate, and track particles using a combination of manual and automated techniques. The associated tracks each represent a unique particle that was further analyzed to estimate its ejection time, 3D trajectory, and velocity, as well as its photometric properties, which were used to compute its brightness, size, and mass. Compiling the aggregate photometric and physical data for all of the particles leads to an estimate of total sample mass lost during the post-TAG imaging sequences. These results further inform an understanding of the sample escape mechanisms and sample loss that occurred before the sample head was stowed in the return capsule on October 28, 2020.

REFERENCES

Arthur, D., and S. Vassilvitskii. “K-means++: The Advantages of Careful Seeding.” SODA ‘07: Proceedings of the Eighteenth Annual ACM-SIAM Symposium on Discrete Algorithms. 2007, pp. 1027–1035.

Blackman, S. S., “Multiple hypothesis tracking for multiple target tracking,” IEEE Aerospace and Electronic Systems Magazine, Vol. 19, No. 1, 2004, pp. 5–18. https://doi.org/10.1109/MAES.2004.1263228.

Calinski, T., and J. Harabasz. “A dendrite method for cluster analysis.” Communications in Statistics. Vol. 3, No. 1, 1974, pp. 1–27.

Chesley, S. R. et al. (2020). Trajectory estimation for particles observed in the vicinity of (101955) Bennu. JGR Planets doi:10.1029/2019JE006363.

DellaGiustina, D. N. & Emery, J. P. et al. (2019). Properties of rubble-pile asteroid (101955) Bennu from OSIRIS-REx imaging and thermal analysis. Nature Astronomy doi:10.1038/s41550-019-0731-1.

Hergenrother, C. W. et al. (2020). Photometry of particles ejected from active asteroid (101955) Bennu, JGR Planets doi:10.1029/2020JE006381.

Lauretta, D. S., Hergenrother, C. W. et al. (2019). Episodes of particle ejection from the surface of the active asteroid (101955) Bennu. Science doi:10.1126/science.aay3544.

Lauretta, D.S. et al. “OSIRIS-REx: Sample Return from Asteroid (101955) Bennu.” Space Science Reviews, Vol. 212, 925–984.

Levesque, M., M. P. Lelievre, “Evaluation of the Iterative Method for Image Background Removal in Astronomical Images,” Defence Research and Development Canada Valcartier (Quebec), 2008.

Pelgrift, J. Y. et al. (2020). Reconstruction of Bennu Particle Events from Sparse Data. Earth and Space Science doi:10.1029/2019EA000938.

Rizk, B. et al., “OCAMS: the OSIRIS-REx Camera Suite.” Space Science Reviews, Vol. 214, No. 1, 2018, article id 26.